A procedure for testing the significance of orbital tuning of the martian polar layered deposits

CrossMark

Michael M. Sori [a,*], J. Taylor Perron [a], Peter Huybers [b], Oded Aharonson [c]

[a] Department of Earth, Atmospheric and Planetary Sciences, Massachusetts Institute of Technology, Cambridge, MA 02139, USA
[b] Department of Earth and Planetary Sciences, Harvard University, Cambridge, MA 02138, USA
[c] Center for Planetary Science, Weizmann Institute of Science, Rehovot, Israel

ABSTRACT

Layered deposits of dusty ice in the martian polar caps have been hypothesized to record climate changes driven by orbitally induced variations in the distribution of incoming solar radiation. Attempts to identify such an orbital signal by tuning a stratigraphic sequence of polar layered deposits (PLDs) to match an assumed forcing introduce a risk of identifying spurious matches between unrelated records. We present an approach for evaluating the significance of matches obtained by orbital tuning, and investigate the utility of this approach for identifying orbital signals in the Mars PLDs. Using a set of simple models for ice and dust accumulation driven by insolation, we generate synthetic PLD stratigraphic sequences with nonlinear time–depth relationships. We then use a dynamic time warping algorithm to attempt to identify an orbital signal in the modeled sequences, and apply a Monte Carlo procedure to determine whether this match is significantly better than a match to a random sequence that contains no orbital signal. For simple deposition mechanisms in which dust deposition rate is constant and ice deposition rate varies linearly with insolation, we find that an orbital signal can be confidently identified if at least 10% of the accumulation time interval is preserved as strata. Addition of noise to our models raises this minimum preservation requirement, and we expect that more complex deposition functions would generally also make identification more difficult. In light of these results, we consider the prospects for identifying an orbital signal in the actual PLD stratigraphy, and conclude that this is feasible even with a strongly nonlinear relationship between stratigraphic depth and time, provided that a sufficient fraction of time is preserved in the record and that ice and dust deposition rates vary predictably with insolation. Independent age constraints from other techniques may be necessary, for example, if an insufficient amount of time is preserved in the stratigraphy.

© 2014 Elsevier Inc. All rights reserved.

1. Introduction

The topographic domes of the north and south polar ice caps on Mars are mostly composed of kilometers-thick layered sedimentary deposits, the polar layered deposits (PLDs), which are exposed in spiraling troughs cut into the caps (Murray et al., 1972; Cutts, 1973; Howard et al., 1982; Byrne, 2009), as shown in Fig. 1. The PLDs were initially seen in images from the Mariner 9 spacecraft (Murray et al., 1972), and were immediately inferred to be composed of atmospherically deposited dust and ice (Cutts, 1973). Since then, the PLDs have been more thoroughly characterized. Carbon dioxide ice and clathrate hydrate have been shown to be compositionally insignificant based on their effects on thermal properties (Mellon, 1996) and bulk strength (Nye et al., 2000).

Water ice dominates dust volumetrically; dust volume composition has an upper limit of 2% in the north polar cap (Picardi et al., 2005) and 10% in the south polar cap (Plaut et al., 2007) according to MARSIS radar transparency data, and ~15% in the south polar cap according to gravity anomalies associated with the area (Zuber et al., 2007; Wieczorek, 2008). Concentrations far smaller than these upper bounds could produce the observed brightness differences (Cutts, 1973). MOLA topography demonstrates that the ice caps are dome-like structures 3–4 km thick (Zuber et al., 1998), with volumes of 1.14 million km^3 for the northern dome (Smith et al., 2001) and 1.6 million km^3 for the southern dome (Plaut et al., 2007). The deposits are locally overlain by seasonal carbon dioxide frost (Smith et al., 2001). Radar soundings from the SHARAD instrument (Phillips et al., 2008) have revealed that large-scale stratigraphy is similar in different parts of the northern ice cap, implying that the PLDs record regional or global climate phenomena rather than local conditions.

* Corresponding author.
  E-mail address: mms18@mit.edu (M.M. Sori).

100 m

100 m
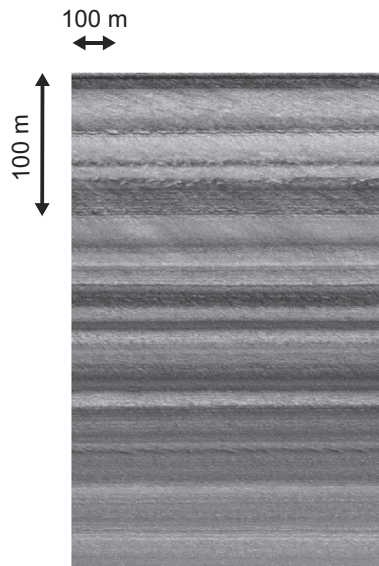
Fig. 1. Mars Orbiter Camera (MOC) Image #M0001754 of a PLD stratigraphic sequence, corrected for topography. The vertical scale corresponds to vertical depth within the PLD sequence, and the horizontal scale corresponds to distance along the outcrop.

Many authors have attempted to constrain the deposition rates of polar ice or dust (Pollack et al., 1979; Kieffer, 1990; Herkenhoff and Plaut, 2000), but these estimates span orders of magnitude. Populations of impact craters on the polar caps provide some constraints, including an estimated mean surface age of 30–100 Myr for the southern PLDs (Koutnik et al., 2002) and an estimated upper limit on the accumulation rate of 3–4 mm/yr for the northern PLDs (Banks et al., 2010). Despite these efforts, the ages of the PLDs remain poorly constrained.

It has been proposed that patterns in the thickness and brightness of these layers, which are thought to result from variable dust concentration in the ice, are controlled by changes in the distribution of solar radiation due to quasi-periodic variations in the planet's spin and orbital characteristics over time, specifically climatic precession, obliquity variation, and eccentricity variation (Murray et al., 1973; Cutts et al., 1976; Toon et al., 1980; Cutts and Lewis, 1982; Howard et al., 1982; Thomas et al., 1992; Laskar et al., 2002; Milkovich and Head, 2005; Milkovich et al., 2008; Fishbaugh et al., 2010; Hvidberg et al., 2012). In this way, the PLDs may record past martian climate.

An analogous argument is often made regarding ice cores or marine sediment cores and Earth's paleoclimate. Some of the variability in marine Pleistocene paleoclimate proxies has been convincingly linked to orbital changes (Hays et al., 1976). However, there is debate about how much of the recorded climate variability was deterministically controlled by Milankovitch cycles (Kominz and Pisias, 1979; Wunsch, 2004). In theory, the problem on Mars should be more tractable than the analogous problem on Earth. The martian atmosphere is orders of magnitude less massive than Earth's, and Mars has not had a surface ocean in the recent past, two factors that should make the martian climate system simpler than the terrestrial one. Mars also experiences larger obliquity and eccentricity variations than Earth (Ward, 1973; Touma and Wisdom, 1993; Laskar et al., 2004), which should make an orbital signal, if present, stronger and perhaps easier to detect.

Despite the likelihood of a simpler climate on Mars, detection of an orbital signal in the PLDs is not a trivial task. The relationship between time and stratigraphic depth in the PLDs is unknown, and is likely nonlinear. There are no absolute ages available for any part of the deposits. Image brightness may contain noise from

image artifacts, inherent noise in the deposition rates of ice and/or dust, and an indirect relationship between visible albedo and PLD composition (Tanaka, 2005; Fishbaugh and Hvidberg, 2006; Herkenhoof et al., 2007; Levrard et al., 2007). Because of these complexities and uncertainties, detection of an orbital signal in the martian PLDs using spacecraft observations poses a considerable challenge (Perron and Huybers, 2009).

The problem of orbital signal detection has been considered almost since the PLDs were first discovered. Given the lack of an absolute chronology, most efforts to interpret the PLDs have focused on modeling or analyzing their stratigraphy. The first study to consider in detail how different PLD formation mechanisms influence the resulting stratigraphy was that of Cutts and Lewis (1982). They considered two deposition models. In their first model, material composing the major constituent of the PLDs is deposited at a constant rate, and differences between layers are caused by a minor constituent that is deposited at a constant rate only when the obliquity of the planet is below a certain threshold value. In their other model, only one type of material is deposited, but only when the obliquity is below a certain threshold value; layer boundaries correspond to periods with no deposition. Although these models are highly simplified, their work revealed the sensitivity of PLD stratigraphy to factors such as ice deposition rates and thresholds, and thus hinted at the difficulty of detecting an orbital signal. More recently, Levrard et al. (2007) used a global climate model for Mars to study ice accumulation rates and concluded that formation of PLD layers must indeed be more complex than originally modeled. Hvidberg et al. (2012) built upon the models of Cutts and Lewis with physically plausible mechanisms of ice and dust deposition, and showed that their models could generate synthetic PLD sequences consistent with some stratigraphy observed in the top 500 m of the PLDs.

Other authors have used time series analysis to search for coherent signals in the PLD stratigraphy, particularly signals that may be related to orbital forcing. Milkovich and Head (2005) analyzed spectra of brightness profiles through the north PLDs, and reported the presence of a signal with a 30 m vertical wavelength in the upper 300 m of the PLDs, which they interpreted as a signature of the approximately 51 kyr cycle of the climatic precession. They assumed a linear time–depth relationship, however, and did not evaluate the statistical significance of the signal they identified. Perron and Huybers (2009) expanded this analysis, also assuming a linear time–depth relationship on average, but allowing for local variability ("jitter") in this relationship. They also evaluated the significance of peaks in the PLD spectra with respect to a noise background. Perron and Huybers (2009) found that the PLD spectra closely resemble spectra for autocorrelated random noise, but that many stratigraphic sequences contain intermittent, quasi-periodic bedding with a vertical wavelength of 1.6 m. Subsequent studies have confirmed and refined this measurement of 1.6 m bedding through analyses of higher-resolution imagery and stereo topography (Fishbaugh et al., 2010; Limaye et al., 2012).

These applications of conventional time series analysis techniques have revealed signals within the stratigraphy, but have not been able to conclusively identify evidence of orbital forcing due to the absence of multiple periodic signals with a ratio of wavelengths that matches the expected ratio of orbital periods (Perron and Huybers, 2009). They have also been limited by the assumption of a linear time–depth relationship, a scenario that, while possible, is rare in terrestrial stratigraphic sequences (Sadler, 1981; Weedon, 2003). Thus, while the Mars polar caps do appear to record repeating regional or global climate events, the duration of these events and their relationship to orbitally forced variations in insolation remain unknown.

In studies of terrestrial paleoclimate records, it is common to address the problem of unknown time–depth relationships by

tuning an observed record – adjusting its time model nonuniformly by moving points in the record closer together or further apart – to match an assumed forcing with a known chronology, or by tuning two or more observed records with unknown chronologies to match each other. There have been limited efforts to apply tuning procedures to the Mars PLDs. Laskar et al. (2002) compared the PLD stratigraphy with an insolation time series using an approach in which a portion of the photometric brightness image was stretched to provide an approximate fit to the insolation time series. They analyzed only one image, however, and did not evaluate the goodness of fit statistically. Milkovich et al. (2008) used the signal-matching algorithm of Lisiecki and Lisiecki (2002) to search for stratigraphic correlations between PLDs in different regions of the north polar cap, but did not attempt to tune PLD sequences to match insolation records.

The need to assess the statistical significance of proposed tunings is widespread in the study of terrestrial paleoclimate (Proistosescu et al., 2012) and in other analyses that seek correlations among time series with uncertain chronologies. The essential problem is that any effort to tune records to match one another will produce some agreement, but it is not clear whether this agreement arose by chance, or whether it reveals an underlying relationship. To address this need, methods have been proposed that estimate the significance of a tuned fit between records, generally by comparing the fit between records that are hypothesized to share an underlying relationship with fits to random records that share no underlying relationship with the observed record. This was the general approach adopted by Milkovich et al. (2008) in their effort to correlate PLD stratigraphic sequences with one another.

In this paper, we adapt a statistical procedure for evaluating the significance of orbital tuning that has been successfully applied to terrestrial paleoclimate records and has been shown to be applicable to comparisons between any two time-uncertain series (Haam and Huybers, 2010). That study considered an application where the time series were known to be approximately 9000 years in total; for our application to the martian PLDs, the total duration is much more uncertain but the same statistical methods apply, albeit with the expectation that the power of the method will be lower. Of course, one should also consider any independent age constraints on the PLDs to guide the technique and determine if a resulting match is physically plausible. We use the procedure to compare two data series – insolation as a function of time and composition of strata as a function of depth – and assess the potential for detecting an orbital signal in the Mars polar layered deposits. Our approach is divided into two main steps. First, we construct simplified models for PLD accumulation and drive these models with a martian insolation time series to create synthetic PLD records. We consider three different models, none of which produces a linear time–depth relationship. In the second step, we perform a statistical analysis to determine how reliably we can detect the orbital signal in the synthetic PLD records. The statistical analysis uses a dynamic time warping algorithm to tune the synthetic PLD records to the insolation time series and a Monte Carlo procedure that evaluates the statistical significance of that tuning by applying the same dynamic time warping algorithm to random signals. For each modeled PLD formation mechanism, this procedure yields an estimated confidence level for detection of an orbital signal. We then consider the implications of this analysis for the interpretation of the PLD stratigraphic sequences measured from spacecraft observations, including the prospects for identifying evidence of orbital forcing. The purpose of our work is not to definitively identify the accumulation function controlling PLD formation, but to assess the performance of a technique that can be used to analyze PLD records that do not have a linear depth–age relationship.

2. Polar layered deposit formation models

2.1. Insolation forcing

In the models presented here, hypothetical ice and dust deposition rates expressed as functions of insolation are integrated forward in time to produce synthetic PLD stratigraphic sequences. Changes in the seasonality and global distribution of insolation on Mars are controlled mainly by the planet's climatic precession, obliquity variations, and eccentricity variations (Ward, 1973, 1974, 1992; Touma and Wisdom, 1993; Laskar et al., 2004). The climatic precession of Mars has a period of approximately 51 kyr. The obliquity of Mars varies with an average period of 120 kyr due to variation of the spin axis and is modulated by a 1200 kyr period due to variation of its orbital inclination (Ward, 1973). The eccentricity of Mars's orbit varies with periods of 95 kyr, 99 kyr and 2400 kyr (Laskar et al., 2004).

The evolution of martian orbital parameters over long time intervals is chaotic (Laskar and Robutel, 1993; Touma and Wisdom, 1993). Given the precision with which present-day orbital parameters can be measured, the current solution for insolation over time (Laskar et al., 2004) is accurate for the last 10–20 Myr. We calculate insolation over this interval from the orbital solution of Laskar et al. (2004) using methods described by Berger (1978). Like previous analyses of the PLDs (Laskar et al., 2002), we use the average daily insolation at the north pole on the summer solstice (Fig. 2) as a proxy for the climatic conditions controlling the deposition of polar ice and dust. This assumes that the effect of the axial precession on the magnitude of ice deposition in a given year is less important than the effect of obliquity. As noted above, our objective in this study is to evaluate a procedure for analyzing PLD sequences with nonlinear time–depth relationships, not to identify the exact relationship between insolation and PLD formation, so our results do not rely on the correctness of this assumption.

The orbital solution features a significant reduction in mean obliquity, and therefore summer insolation at the poles, after approximately 5 Ma. Paleoclimate models suggest that polar ice caps would not have been stable before this time (Jakosky et al., 1995; Mischna et al., 2003; Forget et al., 2006; Levrard et al., 2007), which would imply that the PLDs exposed in the upper portions of the ice caps are younger than 5 Ma. However, other studies have estimated the age of the southern PLDs to be an order of magnitude older than this, which may be related to protective lag deposits (Banks et al., 2010). There is an observational constraint from crater counts that yields a maximum age of ~1 Ga on the north polar basal units (Tanaka et al., 2008), and our approach does
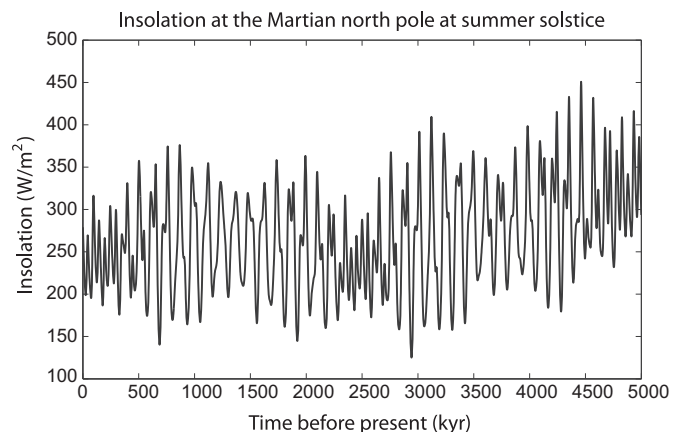

Fig. 2. Martian insolation over the past 5 myr at the north pole on the summer solstice, calculated from the orbital solution of Laskar et al. (2004).

not depend on an estimate of the absolute age of the PLDs. In the models presented here, we only consider the past 5 myr of martian insolation history (Fig. 2).

2.2. Ice and dust accumulation

We consider three classes of PLD formation models, which are illustrated schematically in Fig. 3. Although our models are more complicated than those originally studied by Cutts and Lewis (1982), they are not intended to capture all aspects of the physical processes controlling ice and dust deposition rates. The key attribute of our simple, insolation-driven models is that they produce strata with a nonlinear time–depth relationship, and therefore provide a useful tool for exploring how insolation forcing may be recorded in the PLDs. In each model, dust deposition rate f_{dust} [L/T] is held constant, and ice deposition rate f_{ice} [L/T] is expressed as a simple function of insolation, ϕ (W/m^2). In the first model, ice deposition rate $f_{ice}(\phi)$ varies linearly with insolation. Higher insolation corresponds to slower ice deposition. The insolation value at which no ice is deposited ($f_{ice}(\phi) = 0$) is chosen to be greater than the maximum insolation reached in the past 5 myr, so that $f_{ice}(\phi)$ is always positive, and the resulting PLDs contain no hiatuses in accumulation.

The second model is the same as the first model, except that the insolation at which $f_{ice}(\phi) = 0$ is chosen to be less than the maximum insolation reached in the past 5 myr. For insolation values above this threshold, $f_{ice}(\phi) = 0$. Therefore, for certain time intervals in the past 5 myr, no ice is deposited, and the resulting PLDs contain hiatuses in accumulation.

The third model is the same as the second model, except that $f_{ice}(\phi)$ maintains its linear relationship with insolation at all insolation values, which means that $f_{ice}(\phi)$ is negative for insolation values above the threshold. A negative ice deposition rate corresponds to ablation, which destroys a previously deposited section of the PLD. The resulting PLDs therefore contain hiatuses, as in the second model, but the hiatuses are not limited to time intervals when insolation exceeds a threshold value. Fig. 3 summarizes the ice deposition functions for the three models. All three models can have their parameters adjusted in order to vary the absolute values of their deposition rates. The units of brightness and depth in the
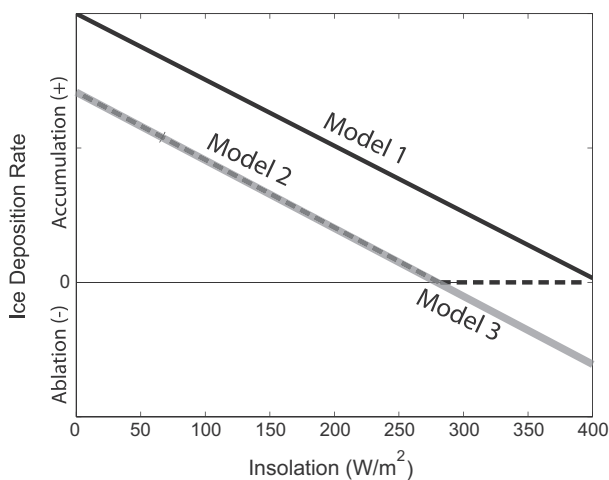
Fig. 3. Ice deposition rate (arbitrary units) as a function of insolation for the three models considered. Model 1 (solid black line) is a simple linear dependence of deposition rate on insolation, with no hiatuses in deposition. Model 2 (dotted line) allows ice deposition rate to drop to zero at high insolation values, creating hiatuses. Model 3 (solid gray line) allows ice deposition rate to become negative at high insolation values, causing alabation of existing layers.

models are arbitrary, so the slopes of the trends relating deposition rate to insolation in Fig. 3 do not affect our tuning procedure.

2.3. Generation of synthetic stratigraphic sequences

For each instance of a model, the insolation time series (Fig. 2) is sampled every 1000 years, for a total of 5000 time steps. At every time step, ice and dust deposition rates are calculated, an increment of ice is deposited using a forward Euler method, and the dust concentration of the ice is calculated as the ratio of the dust and ice deposition rates. This iterative procedure constructs a synthetic PLD stratigraphic sequence consisting of a series of "beds" of unequal thickness and variable dust concentration. Fig. 4 shows examples of outputs for each model class.

The models make a number of simplifications. Dust is assumed to be volumetrically negligible, on the basis of work that suggests an upper limit for dust content of 2% by volume for the northern polar cap (Picardi et al., 2005). Dust is assumed to blow away during hiatuses in ice deposition, such that dust lags do not develop in models with hiatuses or ablation. This assumption is consistent with abundant evidence for eolian sediment transport in the north polar region (Byrne, 2009). We neglect topographic differences involving aspect and shadowing that could potentially cause local variations in deposition rates, based on the observation that large-scale stratigraphy is consistent across the polar ice caps (Phillips et al., 2008). In this study, we have chosen to ignore insolation-induced variations in dust deposition rate, because we expect ice deposition to be more strongly influenced by insolation (Toon et al., 1980). Dust deposition rate is likely to be affected by global dust storms, which may correlate with insolation (Zurek and Martin, 1993), but in the absence of a clear expectation for the relationship between insolation and dust, and given the evidence that atmospheric dustiness varies considerably over intervals much shorter than the periods of orbital changes (Zurek and Martin, 1993), the relation between insolation and ice deposition rate is a logical starting point. Stratigraphic thickness and dust concentrations are presented in arbitrary units, because long-term deposition rates of ice and dust are poorly constrained, with estimates spanning three orders of magnitude (Pollack et al., 1979; Kieffer, 1990; Herkenhoff and Plaut, 2000). This does not pose a problem for the tuning procedure described below, because potential detection of an orbital signal involves consideration of the relative amplitudes and frequencies of stratigraphic signals in PLD records rather than the absolute dust concentrations and stratigraphic distances.

3. Statistical analysis

Our statistical analysis consists of two main components: a dynamic time warping algorithm that tunes a synthetic PLD record in an effort to match the insolation function, and a Monte Carlo procedure that evaluates the statistical significance of the match.

3.1. Orbital tuning by dynamic time warping

Dynamic time warping (DTW) allows for the possibility that the PLDs do not follow a linear time–depth relationship. We use a DTW algorithm proposed by Haam and Huybers (2010) that tunes a record – stretches or contracts its time dimension nonuniformly – to find the optimal match between the record and another time series. The goodness of the match for a given tuning is measured by the covariance between the tuned record and the other time series, and the optimal tuning is the one that maximizes this covariance. In this case, the records are the synthetic PLDs, and they are tuned to match the insolation function.

Model 1

Model 2

Model 2, thresh. 200 W/m^2 Model 2, thresh. 250 W/m^2
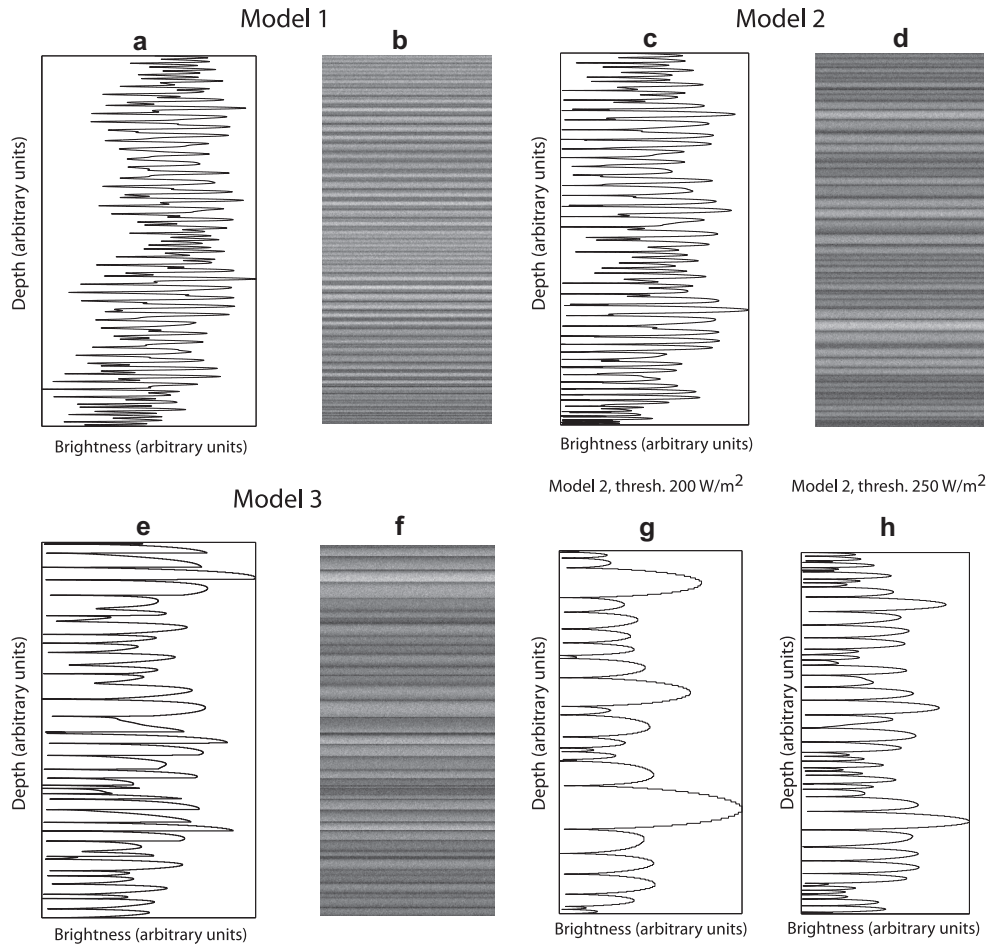
Model 3

Fig. 4. Examples of synthetic PLD stratigraphic sequences produced by the three model classes. Plots in (a, c and e) show dust concentration in arbitrary units as a function of depth in arbitrary units. Images in (b, d and f) show simulated images of the stratigraphy (compare with Fig. 1) created by assuming that brightness scales inversely with dust concentration and adding Gaussian noise. The third model class (e and f), which includes ablation, produces synthetic PLDs most visually similar to actual images. Plots in (g and h) were both produced by the model with hiatuses and no ablation, but with different values of the threshold insolation for ice accumulation: 200 W/m^2 in (g), 250 W/m^2 in (h).

The DTW algorithm tunes the record to the forcing function by using a cost matrix, which is constructed by computing the squared differences between each point in the synthetic record and every point in the insolation function. The resulting matrix of squared differences represents the costs (penalties) of all possible matches between points in the two records. The algorithm then finds the path through the cost matrix that incurs the lowest average cost, starting from an element that corresponds to the top of the PLD record and the estimated time in the insolation function when the uppermost layer was deposited, and ending at an element that corresponds to the bottom of the PLD record and the time in the insolation function when the first layer was deposited. The calculated path represents the tuned record that has the maximum possible covariance with the insolation function. Fig. 5 shows an example of an output of the DTW algorithm with both the tuned and actual time–depth curves. The least-cost path is not required to terminate with the earliest time in the insolation function; since most troughs only expose the uppermost few hundred meters of stratigraphy out of a total of ~2 km, it is likely that exposed deposits only correspond to a fraction of the 5 Myr insolation function. Similarly, the path is not required to start at the present day, because the uppermost strata may have formed some time before the present. However, we expect that the age of the bottom of a PLD sequence is much less certain than the age of the top, so we do not allow the starting point of the least-cost path to vary as freely as the ending point. This is implemented by imposing a

non-zero cost on the leftmost column of the cost matrix and no cost on the rightmost column (Fig. 5). We also impose a non-zero cost on the bottom row because a path traveling along that row would correspond either to the unlikely scenario of a thick layer of ice deposited instantaneously at the present day or to the unphysical scenario of strata that are younger than the present.

3.2. Monte Carlo procedure

The DTW algorithm gives the maximum covariance between a tuned synthetic PLD and the insolation time series, but does not assign a statistical significance to that covariance. The procedure therefore requires an additional step that quantitatively evaluates the null hypothesis that the PLD record is a random time series uncorrelated with insolation, and that the maximum covariance between the PLD and insolation is no better than that obtained by chance. We evaluate this null hypothesis through a Monte Carlo procedure in which random records with statistical characteristics similar to those of the synthetic PLDs are tuned to match the insolation function. For each synthetic PLD, 1000 random records with the same mean, variance, and lag-1 autocorrelation as the synthetic PLD are generated. The DTW procedure then tunes each random record to the insolation record using the same procedure applied to the synthetic PLD, yielding a maximum covariance for each random record. A comparison of the resulting distribution of 1000 maximum covariances with the maximum covariance
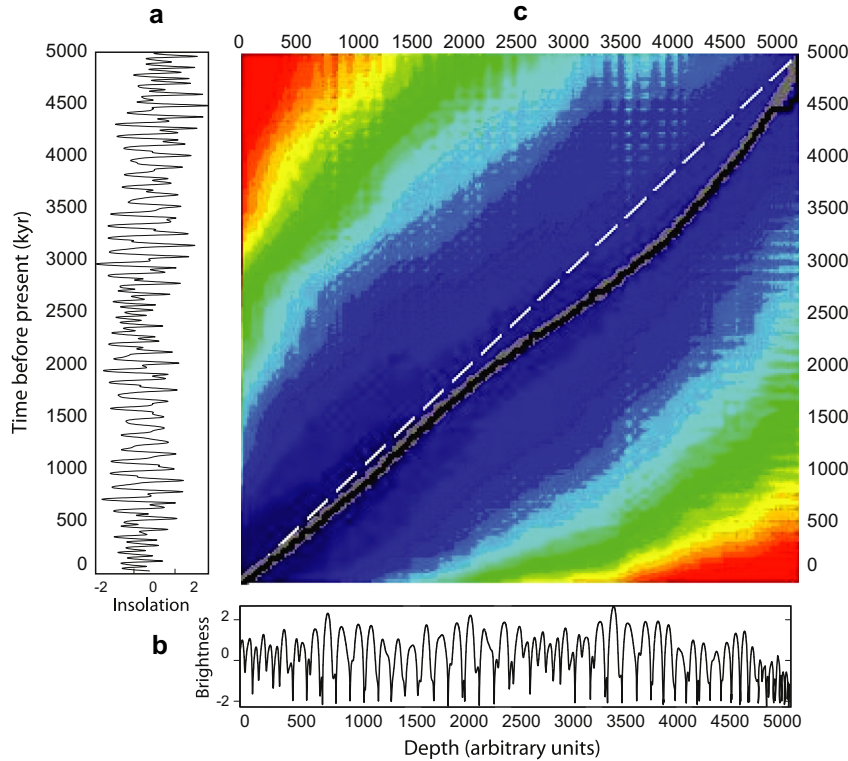
Fig. 5. Output from the dynamic time warping algorithm comparing (a) the last 5 myr of martian insolation history to (b) a synthetic PLD sequence. Both time series are normalized to unit variance. In the model, ice deposition stops (but without ablation) above a threshold insolation of 350 W/m². The square region (c) corresponds to the cost matrix. The black line in (c) shows the path through the cost matrix that incurs the lowest average cost, and represents the tuned synthetic PLD. The colors represent cost, with warm colors indicating areas of higher cost and cool colors indicating areas of lower cost. The dashed line in (c) is simply the diagonal of the cost matrix, which represents a linear time–depth relationship. The gray line in (c) represents the true time–depth relationship for this synthetic PLD. The covariance for this tuning is 0.963 despite the hiatuses in deposition. (For interpretation of the references to color in this figure legend, the reader is referred to the web version of this article.)
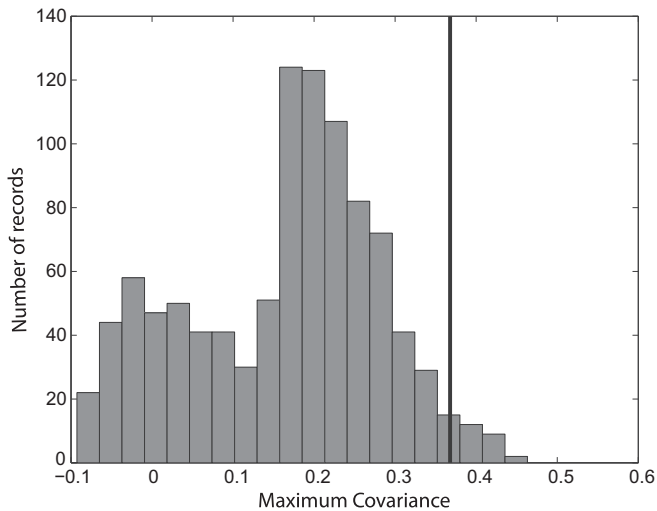
Fig. 6. Histogram showing the distribution of maximum covariances for random records generated from a synthetic PLD where ablation occurs at a threshold insolation value of 270 W/m². The maximum covariance for the synthetic PLD tuned to the insolation record is 0.368 (shown here as the vertical black line), which is greater than 97.2% of the maximum covariances of the random records. We consider this a confident detection of the orbital signal.

between the insolation and synthetic PLD provides a way of gauging the likelihood that the match is not spurious, and therefore the confidence level at which the null hypothesis can be rejected. An example is shown in Fig. 6. We express this confidence level as the percentage of random Monte Carlo records, P_{MC}, that yield a smaller maximum covariance than the synthetic record. If

P_{MC} = 100%, then the synthetic PLD matches insolation better than all random records, and the orbital signal is detected in the synthetic PLD with an extremely high degree of confidence. If P_{MC} = 50%, then the orbital signal is so obscured by the PLD formation mechanism that the tuned match between the PLD and insolation is no better than the median match between a random time series and insolation, and thus there is little confidence that the modeled stratigraphy is related to insolation. Between these two extremes is a range of confidence levels for detection of an orbital signal. This approach provides a way of quantifying the feasibility of detecting an orbital signal given a hypothesized PLD formation mechanism, as well as a way of quantifying the significance of orbital tuning applied to real PLD records, for which the formation mechanism is unknown. Fig. 7 compares dynamic time warping analyses of synthetic PLD models and random time series for one case in which the covariance between insolation and the tuned PLD is substantially higher than for the tuned random time series (Fig. 7a and b) and another in which the PLD and random time series yield comparable covariances (Fig. 7c and d).

4. Results

4.1. Qualitative characteristics of synthetic PLD stratigraphy

Model outputs of synthetic PLD records yield noteworthy trends, even before application of the DTW algorithm and Monte Carlo procedure. In the no-hiatus case, where ice deposition rate varies linearly with insolation and is always positive (Fig. 4a and b), varying the coefficient relating ice deposition rate to insolation changes the absolute values of dust concentration in the resultant
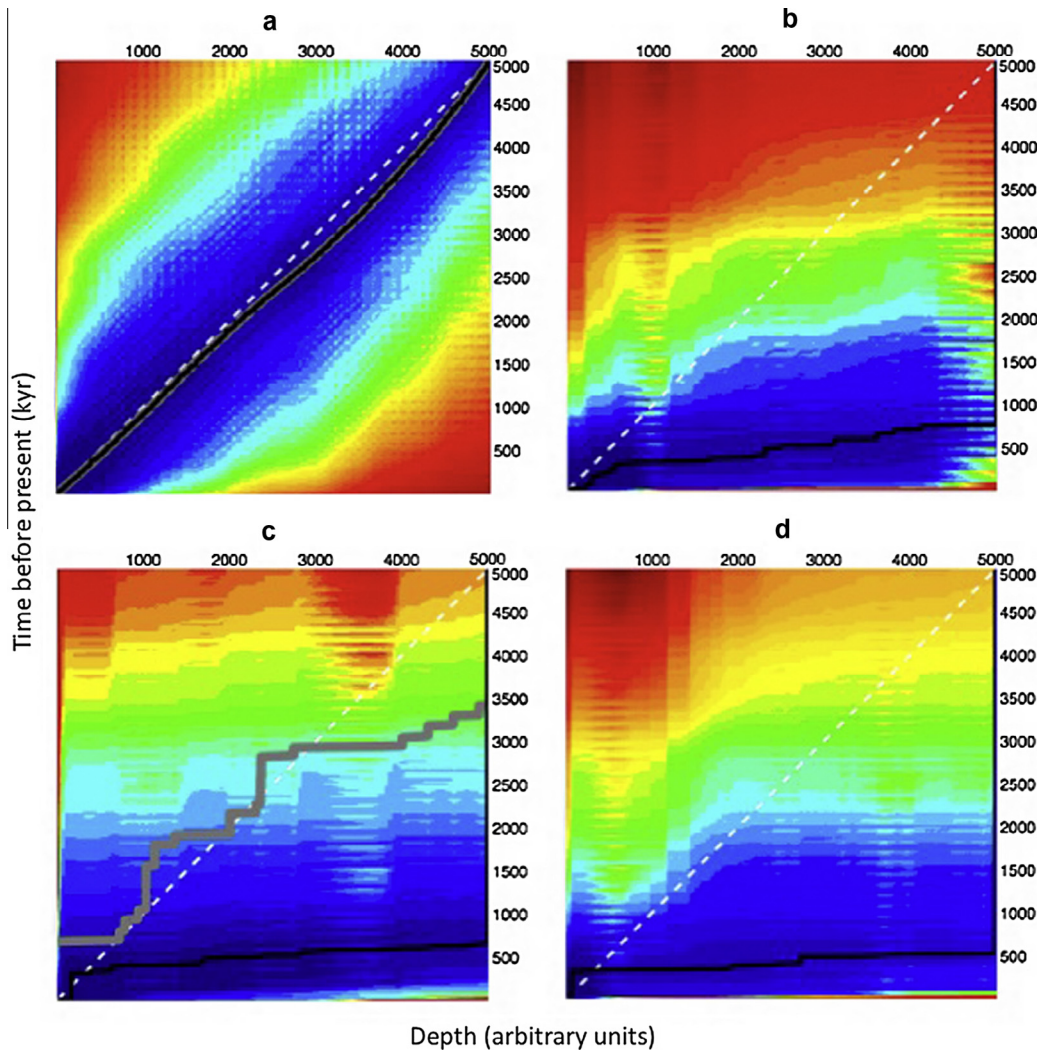
Fig. 7. Cost matrices, as shown in Fig. 5, for four different dynamic time warping analyses. Plot (a) shows a synthetic PLD formed over 5 Myr where ablation occurs at a threshold insolation value of 350 W/m² tuned to a 5 Myr insolation signal. Plot (b) shows a corresponding random PLD tuned to the same signal. Plot (c) shows a synthetic PLD formed over 5 Myr where ablation occurs at a threshold insolation value of 250 W/m² tuned to a 5 Myr insolation signal. Plot (d) shows a corresponding random PLD tuned to the same signal. Note that the tuning in plot (a) is significantly better than that in plot (b), but there is no significant difference between plots (c and d). Solid black lines are the tuned time–depth relationships, gray lines are the true time–depth relationships of the synthetic PLDs, and colors represent higher (warm colors) and lower (cool colors) costs, as in Fig. 5. (For interpretation of the references to color in this figure legend, the reader is referred to the web version of this article.)

stratigraphic sequences, but not the relative frequencies of bedding. The outcome of this simple formation model is therefore qualitatively independent of model parameters.

The relative frequencies of bedding in models that allow hiatuses are also insensitive to changes in the coefficient relating ice deposition rate to insolation (Fig. 4c–f). However, adjusting the threshold insolation value in these models does change the stratigraphy qualitatively, because it influences the fraction of time that is preserved. Fig. 4g and h shows two instances of the model with hiatuses but no ablation, with different thresholds for ice deposition. Note that adjustment of this threshold changes not only the values of dust concentration, but the number of bright peaks as well.

4.2. Detection of orbital signals for different accumulation models

As mentioned in Section 3, a maximum covariance was calculated for each synthetic PLD and was then compared to the maximum covariances obtained for 1000 randomly generated records that shared several statistical properties with the synthetic PLD. For models with no ablation and no hiatuses (Fig. 4a and b), the maximum covariance is close to 1 and is always greater than

the maximum covariances for all randomly generated records (P_{MC} = 100%). Thus, for this simple formation function, we can confidently identify an orbital signal in all cases, despite a nonlinear time–depth relationship that would complicate or preclude detection with conventional time series analysis methods. This result illustrates one of the main benefits of the tuning procedure, and suggests that tuning analyses of the PLDs, combined with an appropriate statistical test, could reveal underlying structure that conventional time series analyses have missed.

For the more complicated models that produce hiatuses (Fig. 4c–f), P_{MC} generally scales with the insolation threshold for ice deposition (Fig. 8a), because higher thresholds result in shorter hiatuses. That is, when less of the insolation time series produces strata that are preserved, the match between the PLDs and insolation is worse, and is less likely to be better than the match to a random record. For sufficiently high insolation thresholds (>225 W/m² for the model with hiatuses but no ablation, and >270 W/m² for the model with ablation), the maximum covariance for the model output is greater than all maximum covariances for random records (P_{MC} = 100%), despite incomplete preservation of the modeled time interval (Fig. 8a). Below those threshold insolation values, P_{MC} decreases as the threshold is lowered. For models without ablation
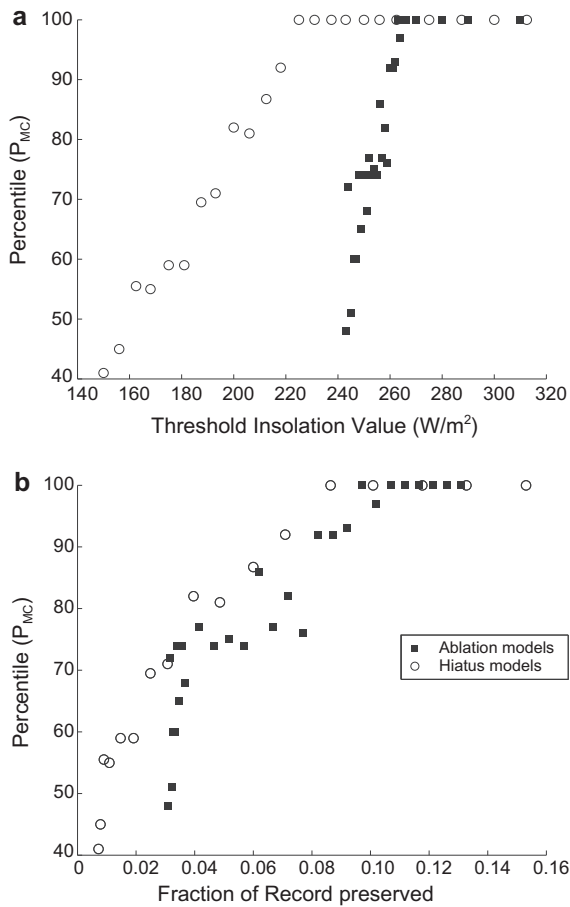
Fig. 8. Percentage of randomly generated time series, P_{MC}, with insolation covariance that is smaller than the insolation covariance of a modeled PLD sequence, as a function of (a) the threshold insolation, and (b) the fraction of the 5 Myr time interval that is preserved in the modeled stratigraphy. Trends for the model with hiatuses but no ablation and the model with hiatuses that do include ablation differ when P_{MC} is compared with the magnitude of the insolation threshold for ice accumulation (a), but overlap when P_{MC} is compared with the fraction of time preserved (b).

but with ice deposition stopping above a threshold insolation value of 222 W/m² an orbital signal can be detected with a 95% degree of confidence. For a threshold insolation value of 174 W/m² or lower, P_{MC} is not significantly higher than 50%, and thus the model output cannot be tuned to an orbital signal better than a random record; detection of an orbital signal is infeasible. For models with ablation above a threshold insolation value of 269 W/m² an orbital signal can be detected with a 95% degree of confidence. For a threshold insolation value of 243 W/m² or lower, P_{MC} is not significantly higher than 50%, and thus the model output cannot be tuned to an orbital signal better than a random record; detection of the signal is infeasible. For a threshold value of 210 W/m² or lower, no PLD record exists – it is all ablated away.

We find that this relationship can be generalized by plotting P_{MC} as a function of the fraction of time preserved in the stratigraphy (Fig. 8b). For the formation models investigated here, the modeled PLDs can be distinguished from random time series ($P_{MC} > 50\%$) even if only a few percent of the modeled time interval is preserved in the stratigraphy, and can be confidently distinguished ($P_{MC} > 90\%$) if approximately 8–10% of the time interval is preserved. Between these extremes, P_{MC} increases approximately linearly with the fraction of time preserved.

We also examined the influence of the total duration of PLD accumulation on the ease of identifying an orbital signal. In

addition to the insolation time series for the past 5 Myr (Fig. 2), we drove the model that allows ablation with the insolation for the past 3 Myr and the past 1 Myr, and performed the same statistical analysis on the model outputs. The results in Fig. 7 demonstrate that, in addition to the dependence on insolation threshold, P_{MC} is higher when the total accumulation interval is longer: depositing the PLDs over a longer period of time makes it easier to detect an orbital influence.

5. Discussion

5.1. Feasibility of identifying an orbital signal through tuning

In general, our results imply that detection of an orbital influence on PLD formation is feasible (though not trivial), even if the relationship between depth and time in the stratigraphy is strongly nonlinear. Indeed, we find that PLD sequences formed by ice and dust deposition models that include no hiatuses in deposition can be distinguished from stochastic time series 100% of the time. While such a deposition model is probably overly simple (see Section 5.3), this result nonetheless emphasizes that a nonlinear time–depth relationship is not an insurmountable complication.

In the more likely scenario that the PLD stratigraphy contains gaps, our analysis provides a framework for determining whether the accumulated record contains enough information to reliably identify orbital influence. Features such as unconformities and crosscutting troughs suggest that the accumulation of the polar stratigraphic record was punctuated by periods of no ice deposition (Tanaka et al., 2008). In models with hiatuses or ablation, the ability to detect orbital signals is a function of the threshold insolation at which ice deposition stops. This result makes intuitive sense: when more of a PLD record is ablated away, it is more difficult to detect the underlying forcing that drove PLD formation. Our procedure identifies a clear, roughly linear relationship between the ease of identifying an orbital influence, as measured by P_{MC}, and the insolation threshold for ice deposition in each model (Fig. 8a). However, these particular values of the insolation threshold should not be interpreted as absolute, because the true relationships between insolation and ice and dust deposition rates are unknown. Instead, we emphasize that the fraction of time preserved in the stratigraphy is the more relevant quantity for determining whether an orbital signal can be confidently detected. The clearest demonstration of this point is that the trends in P_{MC} for the different models collapse to a more uniform trend when plotted against fraction of time preserved (Fig. 8b) rather than the threshold insolation (Fig. 8a).

The other main factor that influences the ease of detecting orbital influence is the total duration of PLD formation. In general, the shorter the time period over which the PLDs form, the more difficult it is to detect an orbital signal in the stratigraphy (Fig. 9). This too makes intuitive sense: a stratigraphic sequence that preserves 50% of 5 myr contains more information than a sequence that preserves 50% of 1 myr, and the additional information makes it easier to distinguish the orbitally driven record from a random record.

5.2. Fraction of time preserved in the polar cap stratigraphy

Although the northern polar cap of Mars is thought to have experienced net accumulation of ice over the past few Myr (Pollack et al., 1979; Kieffer, 1990; Laskar et al., 2002), it is unclear whether the cap is presently in a state of net accumulation or net ablation. If we assume that Mars is in a state of net ablation today, then our models suggest that the current PLDs represent only a small fraction (<10%) of the total record deposited over time. The current insolation at the martian north pole during the summer solstice,
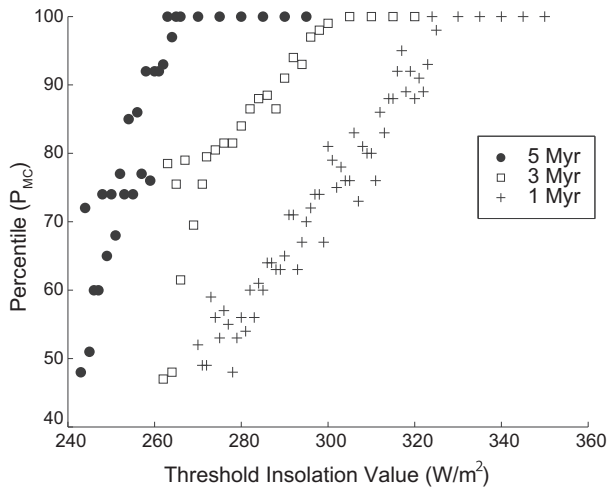
Fig. 9. Percentage of randomly generated time series, P, with insolation covariance that is smaller than the insolation covariance of a modeled PLD sequence, as a function of the insolation threshold for ice accumulation in the model that allows ablation. Different symbols correspond to models in which PLDs are deposited over the past 5, 3, or 1 myr of martian history.

265 W/m², is near the mean insolation for the past 5 Myr of martian history (Fig. 2). Thus, if the PLDs are ablating today, it is likely that they have ablated more often than they have accumulated, and their strata may only record a small fraction of the past 5 Myr. It should be noted, however, that these models assume ablation occurs at a similar rate to ice deposition. If ablation is much slower than ice deposition (which might be the case if, for example, ablation forms a dust lag that inhibits further ablation), the PLDs could record a larger portion of recent martian history, even if the caps are experiencing net ablation today.

5.3. Additional considerations for modeling PLD formation

The objective of this study is to identify the main factors that influence the viability of orbital tuning applied to the PLDs. We therefore have not attempted to formulate a model for PLD accumulation that incorporates all the factors that influence the appearance of the stratigraphy, nor have we attempted an absolute calibration of rate parameters. Nonetheless, given the finding that orbital tuning may indeed be a viable means of identifying the cause of paleoclimate signals preserved in the PLDs, it is important to consider the limitations of, and possible improvements to, the simple models presented here.

Several improvements could be implemented to make the PLD formation models more realistic. In particular, both ice and dust deposition rates could be expressed in terms of a fuller complement of physical variables. Ice deposition rates could take humidity into account. Dust deposition rates could consider the occurrence of global dust storms, which historical observations (Pollack et al., 1979; Toon et al., 1980; Haberle, 1986; Zurek and Martin, 1993) suggest produce a high frequency signal, but which may also include long-term trends related to insolation (Fernandez, 1998). These additional complexities will almost certainly make detection of an orbital signal more difficult, and thus the confidence in detection abilities presented in this study should be interpreted as an upper limit.

Other potential complications are the possibility of stochastic variability in deposition processes and the imperfect relationship between PLD composition and appearance. To explore how these factors influence the orbital tuning procedure, we performed an additional analysis in which the modeled ice deposition rate

includes a stochastic component. Specifically, we added red noise (a random signal in which spectral power P declines with frequency f according to $P \propto f^{-2}$) to the amount of ice deposited in a given time step in our models to generate synthetic PLDs that are not constructed with the assumption of a deterministic relationship between ice deposition rate and insolation. Starting with a model that forms hiatuses when the insolation is 300 W/m² or greater, we varied the amplitude of the noise and produced 100 random realizations of the PLD strata for each value of noise amplitude. We then used the DTW algorithm to calculate the maximum covariance between each modeled stratigraphic sequence and the insolation time series. Fig. 10 shows how the maximum covariance depends on the amplitude of the noise. The addition of red noise to the ice deposition rate changes the maximum covariance in a gradual fashion, suggesting that a non-deterministic relationship between insolation and PLD accumulation does not necessarily prevent the DTW method from identifying an orbital signal.

5.4. Implications for orbital tuning of the observed PLD stratigraphy

Given the probable influence of insolation on the deposition or ablation of water ice, the major constituent of the PLDs, it is likely that the relationship between time and depth in the PLDs is nonlinear, as our simple models predict. One of the main implications of our results is that it may nonetheless be possible to identify evidence of quasi-periodic insolation forcing by applying a tuning procedure like the one described here. Such an analysis could reveal coherent signals in the PLD stratigraphy that would not be detected by conventional time series analysis procedures that assume a linear or nearly linear time–depth relationship (Perron and Huybers, 2009).

The appropriate future direction of this study is to apply the statistical analysis described here to actual images of the martian PLDs. Images obtained by the Mars Orbiter Camera (MOC) on the Mars Global Surveyor spacecraft and the High Resolution Imaging Science Experiment (HiRISE) aboard the Mars Reconnaissance Orbiter can be converted to sequences of brightness vs. depth that can be analyzed with the same procedure as the synthetic sequences of dust concentration studied here (Milkovich and Head,
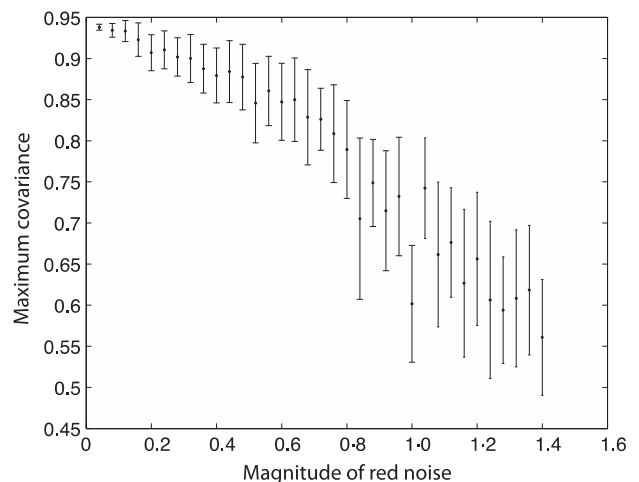
Fig. 10. Effect of adding red noise to the modeled ice deposition rate on the dynamic time warping algorithm's ability to tune the resulting synthetic PLD to the insolation signal. The magnitude of the noise added is the ratio of the variance of the noise to the variance of the ice deposition rate. Each point represents the average maximum covariance of 100 different tunings of a synthetic PLD that contains hiatuses when the insolation reaches a value of 300 W/m² or greater. Error bars are one standard deviation.

2005; Milkovich et al., 2008; Perron and Huybers, 2009; Fishbaugh et al., 2010; Limaye et al., 2012). These sequences should be compared to insolation records of varying time spans, so that we do not assume a certain total age for the sequences from the outset, and with the important consideration that, in the best-case scenario, a match would still only determine the age of the exposed sequence. Such an age would be younger than that of the entire PLDs, which would need to be extrapolated. This procedure can determine if a time-uncertain PLD sequence matches an insolation time series better than random records, but it cannot confirm that such a match reveals the true PLD chronology. In particular, if a PLD sequence containing quasi-periodic signals (Perron and Huybers, 2009; Limaye et al., 2012) is tuned to match an insolation record composed of multiple quasi-periodic signals, there is a possibility that the periods in the sequence will be tuned to match the wrong periods in the forcing. In practice, a procedure such as ours should be applied to PLD records in concert with other lines of evidence (Hinnov, 2013), including climate models (Levrard et al., 2007), polar cap and trough formation models (Smith et al., 2013), and regional stratigraphic analyses, to identify a PLD chronology that is statistically probably and takes into account the relevant geological constraints. It should be noted that conversion of images to brightness-depth sequences introduces an additional source of noise that must be considered (Tanaka, 2005), but recent efforts to quantify these uncertainties have found them to be modest (Limaye et al., 2012). The dynamic time warping procedure we have applied to brightness records can in principle be applied to other proxies for PLD composition, such as sequences of slope or roughness vs. depth, or composite records incorporating both brightness and topographic information. Thus, for any possible identification of an orbital signal in the PLDs, the statistical procedure presented here can yield a quantitative estimate of the likelihood of a spurious match. If the PLDs preserve a sizeable fraction of the total accumulation time, and the deposition rates of ice and dust are sufficiently deterministic, it may well be possible to detect an orbital signal, if one is present.

6. Conclusions

We use a statistical procedure that evaluates the significance of time series tuning to examine the feasibility of detecting an influence of orbital variations on the polar stratigraphy of Mars. We apply the procedure to synthetic stratigraphic sequences generated by simple formation models for the martian polar layered deposits, and find that detection of an orbital signal in the resulting stratigraphy is feasible, though not trivial. Models in which ice deposition rate varies linearly with insolation produce stratigraphy in which orbital signals are easily detected with the tuning procedure, despite a nonlinear relationship between depth and time that can foil conventional time series analysis methods. For more complicated models of ice deposition, detection ability depends strongly on the threshold insolation at which ice deposition stops or an ablation episode begins, and more generally, on the fraction of total formation time preserved in the strata. Improved constraints on ice and dust deposition rates on Mars would permit a more definitive assessment of whether detection of an orbital signal in the PLDs is feasible, but our analysis does not reveal the problem to be necessarily intractable at the current state of knowledge. HiRISE images should be adequate to identify evidence of an orbital influence if PLD formation is controlled by a sufficiently simple mechanism and sufficient time preserved. We find that when too little time is preserved in the stratigraphy, confident identification of an orbital signal may be impossible without absolute ages, even given simple formation scenarios and no matter the quality of the spacecraft images.

References

Banks, M.E. et al., 2010. Crater population and resurfacing of the martian north polar layered deposits. J. Geophys. Res. 115, E08006. http://dx.doi.org/10.1029/2009JE003523.

Berger, A.L., 1978. Long-term variations of daily insolation and Quaternary climatic changes. J. Atmos. Sci. 35, 2362–2367.

Byrne, S., 2009. The polar deposits of Mars. Annu. Rev. Earth Planet. Sci. 37, 535–560.

Cutts, J.A., 1973. Nature and origin of layered deposits of the martian polar region. J. Geophys. Res. 78, 4231–4249.

Cutts, J.A., Lewis, B.H., 1982. Models of climate cycles recorded in martian polar layered deposits. Icarus 50, 216–244.

Cutts, J.A., Blasius, K.R., Briggs, G.A., Carr, M.H., Greeley, R., Masursky, H., 1976. North polar region of Mars: Imaging results from Viking 2. Science 194, 1329–1337.

Fernandez, W., 1998. Martian dust storms: A review. Earth, Moon, Planets 77, 19–46.

Fishbaugh, K.E., Hvidberg, C.S., 2006. Martian north polar layered deposits stratigraphy: Implications for accumulation rates and flow. J. Geophys. Res. 111, E06012. http://dx.doi.org/10.1029/2005JE002571.

Fishbaugh, K.E. et al., 2010. First high-resolution stratigraphic column of the martian north polar layered deposits. Geophys. Res. Lett. 37, L07201. http://dx.doi.org/10.1029/2009GL041642.

Forget, F., Haberle, R.M., Montmessin, F., Levrard, B., Head, J.W., 2006. Formation of glaciers on Mars by atmospheric precipitation at high obliquity. Science 311, 368–371.

Haam, E., Huybers, P., 2010. A test for the presence of covariance between time-uncertain series of data with application to the Dongge Cave speleothem and atmospheric radiocarbon records. Paleoceanography 25, PA2209. http://dx.doi.org/10.1029/2008PA001713.

Haberle, R.M., 1986. Interannual variability of global dust storms on Mars. Science 234, 459–461.

Hays, J.D., Imbrie, J., Shackleton, N.J., 1976. Variations in the Earth's orbit: Pacemaker of the Ice Ages. Science 194, 1121–1132.

Herkenhoff, K., Plaut, J.J., 2000. Surface ages and resurfacing rates of the polar layered deposits on Mars. Icarus 144, 243–253.

Herkenhoof, K.E., Byrne, S., Russell, P.S., Fishbaugh, K.E., McEwen, A.S., 2007. Meter-scale morphology of the north polar region of Mars. Science 317, 1711–1715.

Hinnov, L.A., 2013. Cyclostratigraphy and its revolutionizing applications in the Earth and planetary sciences. Geol. Soc. Am. Bull. 125, 1703–1734.

Howard, A.D., Cutts, J.A., Blasius, K.R., 1982. Stratigraphic relationships between martian polar cap deposits. Icarus 50, 161–215.

Hvidberg, C.S., Fishbaugh, K.E., Winstrup, M., Svensson, A., Byrne, S., Herkenhoff, K.E., 2012. Reading the climate record of the martian polar layered deposits. Icarus 221, 405–419.

Jakosky, B.M., Henderson, B.G., Mellon, M.T., 1995. Chaotic obliquity and the nature of the martian climate. J. Geophys. Res. 100, 1579–1594.

Kieffer, H.H., 1990. H_2O grain size and the amount of dust in Mars residual north polar cap. J. Geophys. Res. 95, 1481–1493.

Kominz, M.A., Pisias, N.G., 1979. Pleistocence climate: Deterministic or stochastic? Science 204, 171–173.

Koutnik, M., Byrne, S., Murray, B., 2002. South polar layered deposits of Mar: The cratering record. J. Geophys. Res. 107, 5100. http://dx.doi.org/10.1029/2001JE001805.

Laskar, J., Robutel, P., 1993. The chaotic obliquity of the planets. Nature 361, 608–612.

Laskar, J., Levrard, B., Mustard, J.F., 2002. Orbital forcing of the martian polar layered deposits. Nature 419, 375–377.

Laskar, J., Correia, A.C.M., Gastineau, M., Joutel, F., Levrard, B., Robutel, P., 2004. Long term evolution and chaotic diffusion of the insolation quantities of Mars. Icarus 170, 343–364.

Levrard, B., Forget, F., Montmessin, F., Laskar, J., 2007. Recent formation and evolution of northern martian polar layered deposits as inferred from a global climate model. J. Geophys. Res. 112, E06012. http://dx.doi.org/10.1029/2006JE002772.

Limaye, A.B.S., Aharonson, O., Perron, J.T., 2012. Detailed stratigraphy and bed thickness of the Mars north and south polar layered deposits. J. Geophys. Res.: Planets 117, E06009.

Lisiecki, L.E., Lisiecki, P.A., 2002. Application of dynamic programming to the correlation of paleoclimate records. Paleoceanography 17 (D4), 1049. http://dx.doi.org/10.1029/2001PA000733.

Mellon, M.T., 1996. Limits on the CO_2 content of the martian polar layered deposits. Icarus 124, 268–279.

Milkovich, S.M., Head III, J.W., 2005. North polar cap of Mars: Polar layered deposit characterization and identification of a fundamental climate signal. J. Geophys. Res. 110, E01005. http://dx.doi.org/10.1029/2004JE002349.

Milkovich, S.M., Head, J.W., Neukum, G.the HRSC Co-Investigator Team, 2008. Stratigraphic analysis of the northern polar layered deposits of Mars: Implications for recent climate history. Planet. Space Sci. 56 (2), 266–288.

Mischna, M.A., Richardson, M.I., John Wilson, R., McCleese, D.J., 2003. On the orbital forcing of martian water and CO_2 cycles: A general circulation model study with simplified volatile schemes. J. Geophys. Res. 108 (E6), 5062. http://dx.doi.org/10.1029/2003JE002051.

Murray, B.C., Soderblom, L.A., Cutts, J.A., Sharp, R.P., Milton, D.J., Leighton, R.B., 1972. Geological framework of the south polar region of Mars. Icarus 17, 328–345.

Murray, B.C., Ward, W.R., Yeung, S.C., 1973. Periodic insolation variations on Mars. Science 180, 638–640.

Nye, J.F., Durham, W.B., Schenk, P.M., Moore, J.M., 2000. The instability of a south polar cap on Mars composed of carbon dioxide. Icarus 144, 449–455.

Perron, J.T., Huybers, P., 2009. Is there an orbital signal in the polar layered deposits on Mars? Geology 37, 155–158.

Phillips, R.J. et al., 2008. Mars north polar deposits: Stratigraphy, age, and geodynamical response. Science 320, 1182–1185.

Picardi, G. et al., 2005. Radar soundings of the subsurface of Mars. Science 310, 1925–1928.

Plaut, J.J. et al., 2007. Subsurface radar sounding of the south polar layered deposits of Mars. Science 316, 92–96.

Pollack, J.B., Colburn, D.S., Flasar, F.M., Kahn, R., Carlston, C.E., Pidek, D.G., 1979. Properties and effects of dust particles suspended in the martian atmosphere. J. Geophys. Res. 84, 2929–2945.

Proistosescu, C., Huybers, P., Maloof, A.C., 2012. To tune or not to tune: Detecting orbital variability in Oligo-Miocene climate records. Earth Planet. Sci. Lett. 325–326, 100–107.

Sadler, P.M., 1981. Sediment accumulation rates and the completeness of stratigraphic sections. J. Geol. 89, 569–584.

Smith, D.E., Zuber, M.T., Neumann, G.A., 2001. Seasonal variations of snow depth of Mars. Science 294, 2141–2145.

Smith, I.B., Holt, J.W., Spiga, A., Howard, A.D., Parker, G., 2013. The spiral troughs of Mars as cyclic steps. J. Geophys. Res.: Planets 118, 1835–1857.

Tanaka, K.L., 2005. Geology and insolation-driven climatic history of Amazonian north polar materials on Mars. Nature 437, 991–994.

Tanaka, K.L. et al., 2008. North polar region of Mars: Advances in stratigraphy, structure, and erosional modification. Icarus 196, 318–358.

Thomas, P. et al., 1992. Polar deposits of Mars. In: Kieffer, H.H. et al. (Eds.), Mars. University of Arizona Press, Tucson, pp. 767–795.

Toon, O.B., Pollack, J.B., Ward, W., Burns, J.A., Bilski, K., 1980. The astronomical theory of climatic change on Mars. Icarus 44, 552–607.

Touma, J., Wisdom, J., 1993. The chaotic obliquity of Mars. Science 259, 1294–1297.

Ward, W.R., 1973. Large-scale variations in the obliquity of Mars. Science 181, 260–262.

Ward, W.R., 1974. Climatic variations on Mars: 1. Astronomical theory of insolation. J. Geophys. Res. 79, 3375–3386.

Ward, W.R., 1992. Long-term orbital and spin dynamics of Mars. In: Kieffer, H.H. et al. (Eds.), Mars. University of Arizona Press, Tucson, pp. 298–320 (Chapter 9).

Weedon, G., 2003. Time-Series Analysis and Cyclostratigraphy. Cambridge University Press, Cambridge.

Wieczorek, M.A., 2008. Constraints on the composition of the martian south polar cap from gravity and topography. Icarus 196, 506–517.

Wunsch, C., 2004. Quantitative estimate of the Milankovitch-forced contribution to observed Quaternary climate change. Quatern. Sci. Rev. 23, 1001–1012.

Zuber, M.T. et al., 1998. Observations of the north polar region of Mars from the Mars orbiter laser altimeter. Science 282, 2053–2060.

Zuber, M.T. et al., 2007. Density of Mars' south polar layered deposits. Science 300, 299–303.

Zurek, R., Martin, L., 1993. Interannual variability of planet-encircling dust storms on Mars. J. Geophys. Res. 98, 3247–3259.